Pergamon

Int. J. Heat Mass Transfer. Vol. 39, No. 4, pp. 761–769, 1996

0017-9310/96 $15.00+0.00

0017-9310(95)00161-1

Numerical analysis of heat transfer in an air-filled bayonet tube under laminar conditions

H. MINHAS and G. S. H. LOCK

Department of Mechanical Engineering, University of Alberta, Edmonton, Alberta, Canada T6G 2G8

(*Received* 24 *August* 1994 *and in final form* 18 *April* 1995)

Abstract—The paper provides details of a numerical study of the bayonet tube under steady, laminar conditions when the fluid is air. Attention is focused on the heat transfer characteristics of the tube. The data constitute a systematic investigation of the effect of the principal parameters on the overall heat transfer rate, represented by a Nusselt number. Specifically discussed are the effects of Reynolds number, length-diameter ratio, the ratio of annular to inner tube area, the ratio of the end clearance to the tube diameter, and the Rayleigh number. Comparisons with experimental data are also made.

1. INTRODUCTION

The bayonet tube is a simple, refluent heat exchanger. As shown in Fig. 1, it is constructed from two concentric tubes, one end of the inner tube reaching close to the sealed end of the outer one. Fluid flowing within and towards the open end of the inner tube is thus constrained to return along the annular gap formed between the two tubes. The system has found extensive use in situations where the medium to be heated or cooled is either too large to be treated in its entirety or is readily accessible from one side only. The medium is then penetrated by insertion of bayonet tubes, in contrast to the more common arrangement of tubes crossing back and forth. The device is discussed more extensively by Lock [1].

In a geophysical context, the bayonet tube may be used to penetrate the earth's surface. In regions

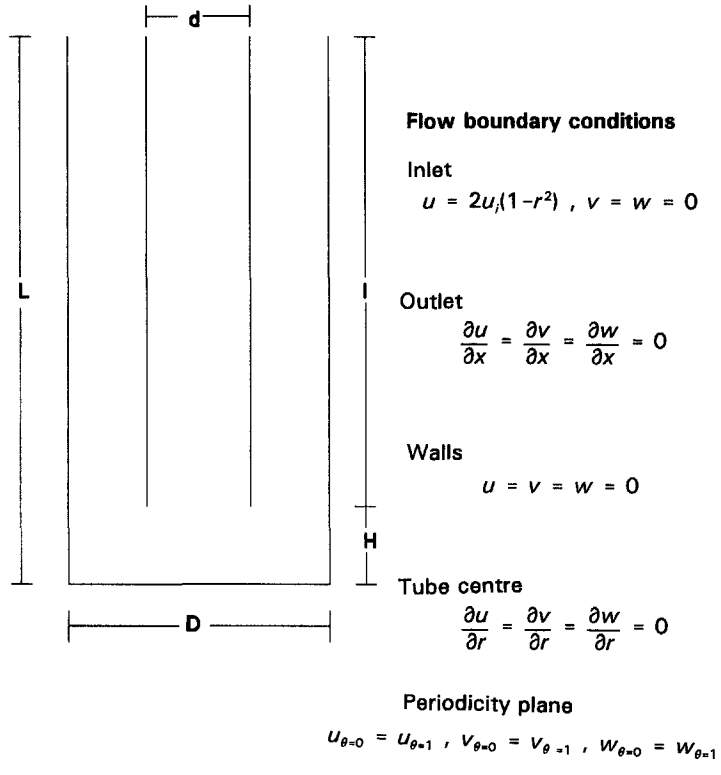

Fig. 1. Dimensions of the bayonet tube.

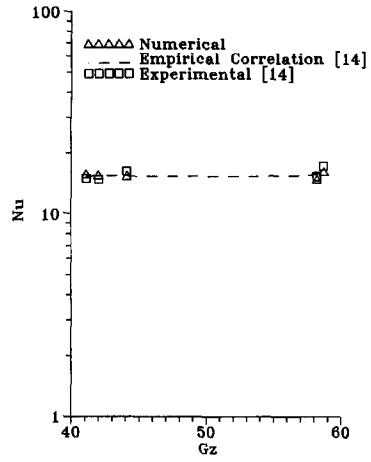

Fig. 2. Mixed convection in a vertical isothermal pipe.

24×24 grid. The heat transfer data are believed to be comparable in accuracy.

For the bayonet tube, the same convergence criterion was used. However, a $41 \times 41 \times 20$ grid was adopted because two pipes are being considered. It was anticipated that a finer grid was needed to accommodate a more complex flow field. An optimum relaxation factor of 0.72 was again used. The program was first run at the "standard", or reference, parametric values used by Lock and Wu [10]: $Re' = 900$, $L/D = 20$, $F_i/F_a = 0.474$ and $H/D = 1$ represent practical operational parameters for a bayonet tube. Test runs with a grid of $61 \times 61 \times 40$ indicated a Nusselt number change of less than 2%, while the time taken to run the program was increased by more than 10%. The percentage mass error between the inlet and the outlet was still less than 0.6%. The results were spot checked for uniqueness by using different initial fields. The solutions remained unchanged.

4. DISCUSSION OF RESULTS

In Fig. 3, the heat flux is plotted as a function of distance $X' = (L-X)/D$, where X is the axial distance and L the outer tube length. A transition from clearance to annular flow occurs between $X' = 0.6$ and 1. In transitional region a local minimum exists corresponding to stagnation point at the wall [11, 15]. Slightly further downstream of the stagnation region gradual reacceleration of the flow creates a local maximum at $H/D \approx 1$. After this the flow becomes fully developed again.

The effect of the principal bayonet tube parameters on the overall heat transfer rate was examined systematically. Each parameter was considered separately, the other parameters being held constant at the reference values. Results are plotted using these parameters. Curves fitted through discrete numerical points employ a cubic spline.

4.1. *Effect of Reynolds number*

As expected, the Nusselt number was found to increase monotonically with Reynolds number, Re', as shown in Fig. 4. Numerical prediction lies within the experimental error range of $\pm 10\%$. In view of the abrupt change in direction it is unlikely the flow would remain laminar up to a Reynolds number of 2500; the results were arbitrarily truncated at $Re' = 1200$.

The temperature field for the widely separated values of $Re' = 100$ and 1000 is represented in Fig. 5; only the five lowest radii of the tube are shown. It is interesting to note the thickness of the thermal boundary layer in the annulus as the Reynolds number decreases. With the inner tube being taken as a perfect conductor, heat may penetrate into the incoming fluid thereby increasing it's temperature. This evidently occurs at $Re' = 100$ but is almost absent at $Re' = 1000$. The effect of the flow details in the clearance zone [11, 15] appears to be very small under these conditions.

4.2. *Effect of length:diameter ratio*

The length:diameter ratio, L/D, also exerts a strong influence on the heat transfer rate. As shown in Fig. 6,

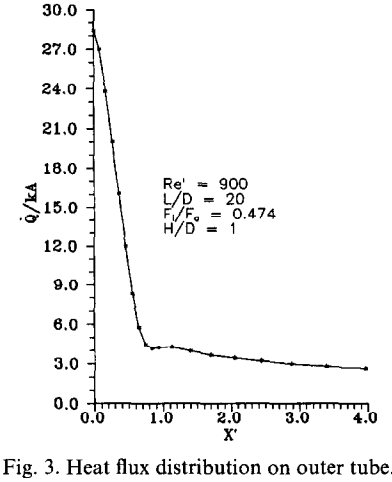

Fig. 3. Heat flux distribution on outer tube.

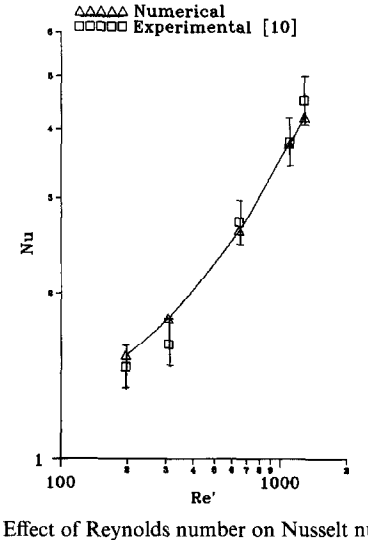

Fig. 4. Effect of Reynolds number on Nusselt number.

$$u\frac{\partial v}{\partial x}+v\frac{\partial v}{\partial r}+\frac{w}{r}\frac{\partial v}{\partial \theta}=-4K^2\frac{\partial p}{\partial r}+\frac{1}{ReK}\frac{\partial^2 v}{\partial x^2}+\frac{4K}{Re}\frac{1}{r}\frac{\partial}{\partial r}\left(r\frac{\partial v}{\partial r}\right)+\frac{K}{\pi^2 Re}\frac{1}{r^2}\frac{\partial^2 v}{\partial \theta^2}-\frac{4K}{Re}\frac{v}{r^2}-\frac{8K}{Re}\frac{1}{r^2}\frac{\partial w}{\partial \theta}+4\pi^2\frac{w^2}{r} \quad (3)$$

$$u\frac{\partial w}{\partial x}+v\frac{\partial w}{\partial r}+\frac{w}{r}\frac{\partial w}{\partial \theta}=-\frac{K^2}{\pi^2}\left(\frac{1}{r}\frac{\partial p}{\partial \theta}\right)+\frac{1}{ReK}\frac{\partial^2 w}{\partial x^2}+\frac{4K}{Re}\frac{1}{r}\frac{\partial}{\partial r}\left(r\frac{\partial w}{\partial r}\right)+\frac{K}{\pi^2 Re}\frac{1}{r^2}\frac{\partial^2 w}{\partial \theta^2}-\frac{4K}{Re}\frac{w}{r^2}+\frac{2K}{\pi^2 Re}\frac{1}{r^2}\frac{\partial v}{\partial \theta}-\left(\frac{vw}{r}\right) \quad (4)$$

$$\frac{1}{r}\frac{\partial}{\partial x}(ru\phi)+\frac{1}{r}\frac{\partial}{\partial r}(rv\phi)+\frac{1}{r}\frac{\partial}{\partial \theta}(w\phi)=\frac{1}{RePrK}\left(\frac{\partial^2\phi}{\partial x^2}\right)+\frac{4K}{RePr}\frac{1}{r}\frac{\partial}{\partial r}\left(r\frac{\partial \phi}{\partial r}\right)+\frac{K}{\pi^2 RePr}\frac{1}{r^2}\frac{\partial^2\phi}{\partial \theta^2} \quad (5)$$

where, since $U^c = 4Kv/D$

$$Re=\frac{\left(\frac{4Kv}{D}\right)D}{v}=4K \quad \text{and} \quad Ra=\beta g\frac{D^3(T_w-T_0)}{v\alpha}.$$

The tube diameter ratio D/d does not appear explicitly above; it is incorporated implicitly through the equations given in Section 2.2.

A parabolic velocity profile was assumed at the entrance to the inner tube. The velocity at all walls was taken to be zero. Fluid inlet and outer tube wall temperatures were set as isothermals, but the bottom of the outer tube was taken to be insulated. Temperature conditions were therefore the same as the experiments of Lock and Wu [10]. The inner tube was taken to be a perfect conductor of zero thickness. Symmetry and periodicity were assumed at the tube centre and periodicity plane ($\Theta = 0, 2\pi$), respectively. At the tube exit, a Neumann boundary condition (zero axial gradient) was set for both temperature and velocity.

2.2. *Definitions*

The results given below are expressed in terms of the following parameters, divided into three categories.

2.2.1. *Geometry.*

(1) Length:diameter ratio: L/D, where L and D are the length and diameter, respectively, of the outer tube.

(2) Area ratio: F_i/F_a, where F_i and F_a are the inner tube and annulus areas, respectively.

(3) Clearance ratio: H/D, where H is the end clearance of the inner tube.

2.2.2. *Flow rate.* Reynolds number: following Lock and Wu [11], the Reynolds number is defined by

$$Re'=\frac{4\dot{m}D}{\rho\pi v(D+d)d}. \quad (6)$$

This was chosen to accommodate the limiting cases of $d \ll D$ and $D \approx d$, given that $(d_0 - d_i) \ll D$.

2.2.3. *Buoyancy.* Rayleigh number:

$$Ra'=\beta g\frac{(D-d)^3(T_w-T_0)}{v\alpha}. \quad (7)$$

This emphasizes the gap $(D-d)$ where most of the heat transfer is expected to occur. The parameter $Ra'(D-d)/L$ which varies between 0.21 and 216.46 indicates the natural convection regime [1].

The above parameters may be expected to influence the overall system performance, as measured by the Nusselt number, Nu, defined in terms of the mean fluid temperature difference between the inlet to the inner tube and outlet from the annulus. The Nusselt number is thus given by:

$$Nu=\frac{\dot{Q}(D-d)}{\pi kDL(T_w-T_f)} \quad (8)$$

where

$$T_f=\frac{T_0+T_b}{2},$$

T_0 and T_b being the fluid bulk temperatures at the inlet and outlet, respectively.

3. NUMERICAL FORMULATION AND VALIDATION

The numerical simulation was done using the algorithm of Patankar [12] in the SIMPLE-C version [13]. The program was validated for steady, laminar, constant property, axisymmetric upward air flow in a straight, vertical, isothermal pipe with no inner tube. A representative length:diameter ratio of 16 was used. Using a relaxation factor of 0.72, the convergence was defined by successive agreement of averaged values of the dependent variables to within 1%: agreement was usually better than this. As expected, the percentage mass error between the inlet and outlet decreased with grid size. Based on a comparative study of different grid sizes, a 24×24 grid was chosen. The percentage mass error between the inlet and outlet for this grid was then less than 0.6%.

Heat transfer accuracy was checked by obtaining Nusselt number ($Nu = h_{lm}d/k$) data at different Graetz numbers ($Gz = \dot{m}c_p/kL$) in the empty pipe. The results are compared with the experimental data [14] and an empirical correlation [14] in Fig. 2. The numerical results are within $\pm 5\%$ of the experimental data and the empirical correlation. Unfortunately, no error range was specified in the above-mentioned experiments. Solutions of a hydraulic study [15] indicate frictional data to be accurate to within 1% for the

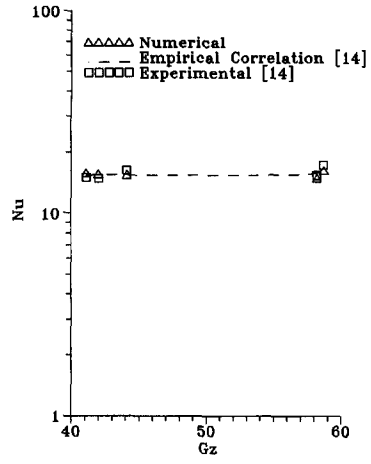

Fig. 2. Mixed convection in a vertical isothermal pipe.

24×24 grid. The heat transfer data are believed to be comparable in accuracy.

For the bayonet tube, the same convergence criterion was used. However, a $41 \times 41 \times 20$ grid was adopted because two pipes are being considered. It was anticipated that a finer grid was needed to accommodate a more complex flow field. An optimum relaxation factor of 0.72 was again used. The program was first run at the "standard", or reference, parametric values used by Lock and Wu [10]: $Re' = 900$, $L/D = 20$, $F_i/F_a = 0.474$ and $H/D = 1$ represent practical operational parameters for a bayonet tube. Test runs with a grid of $61 \times 61 \times 40$ indicated a Nusselt number change of less than 2%, while the time taken to run the program was increased by more than 10%. The percentage mass error between the inlet and the outlet was still less than 0.6%. The results were spot checked for uniqueness by using different initial fields. The solutions remained unchanged.

4. DISCUSSION OF RESULTS

In Fig. 3, the heat flux is plotted as a function of distance $X' = (L-X)/D$, where X is the axial distance and L the outer tube length. A transition from clearance to annular flow occurs between $X' = 0.6$ and 1. In transitional region a local minimum exists corresponding to stagnation point at the wall [11, 15]. Slightly further downstream of the stagnation region gradual reacceleration of the flow creates a local maximum at $H/D \approx 1$. After this the flow becomes fully developed again.

The effect of the principal bayonet tube parameters on the overall heat transfer rate was examined systematically. Each parameter was considered separately, the other parameters being held constant at the reference values. Results are plotted using these parameters. Curves fitted through discrete numerical points employ a cubic spline.

4.1. *Effect of Reynolds number*

As expected, the Nusselt number was found to increase monotonically with Reynolds number, Re', as shown in Fig. 4. Numerical prediction lies within the experimental error range of $\pm 10\%$. In view of the abrupt change in direction it is unlikely the flow would remain laminar up to a Reynolds number of 2500; the results were arbitrarily truncated at $Re' = 1200$.

The temperature field for the widely separated values of $Re' = 100$ and 1000 is represented in Fig. 5; only the five lowest radii of the tube are shown. It is interesting to note the thickness of the thermal boundary layer in the annulus as the Reynolds number decreases. With the inner tube being taken as a perfect conductor, heat may penetrate into the incoming fluid thereby increasing it's temperature. This evidently occurs at $Re' = 100$ but is almost absent at $Re' = 1000$. The effect of the flow details in the clearance zone [11, 15] appears to be very small under these conditions.

4.2. *Effect of length:diameter ratio*

The length:diameter ratio, L/D, also exerts a strong influence on the heat transfer rate. As shown in Fig. 6,

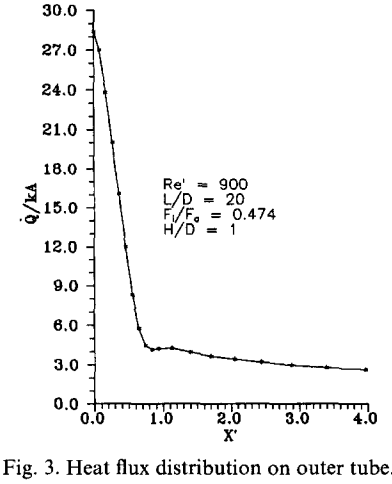

Fig. 3. Heat flux distribution on outer tube.

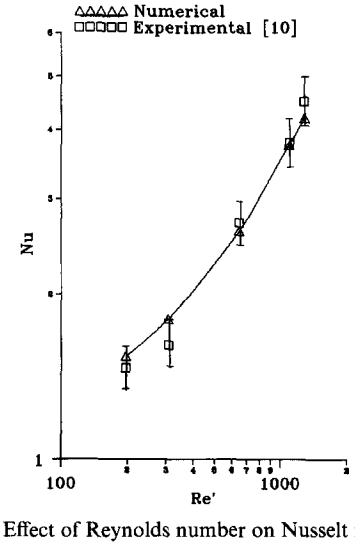

Fig. 4. Effect of Reynolds number on Nusselt number.

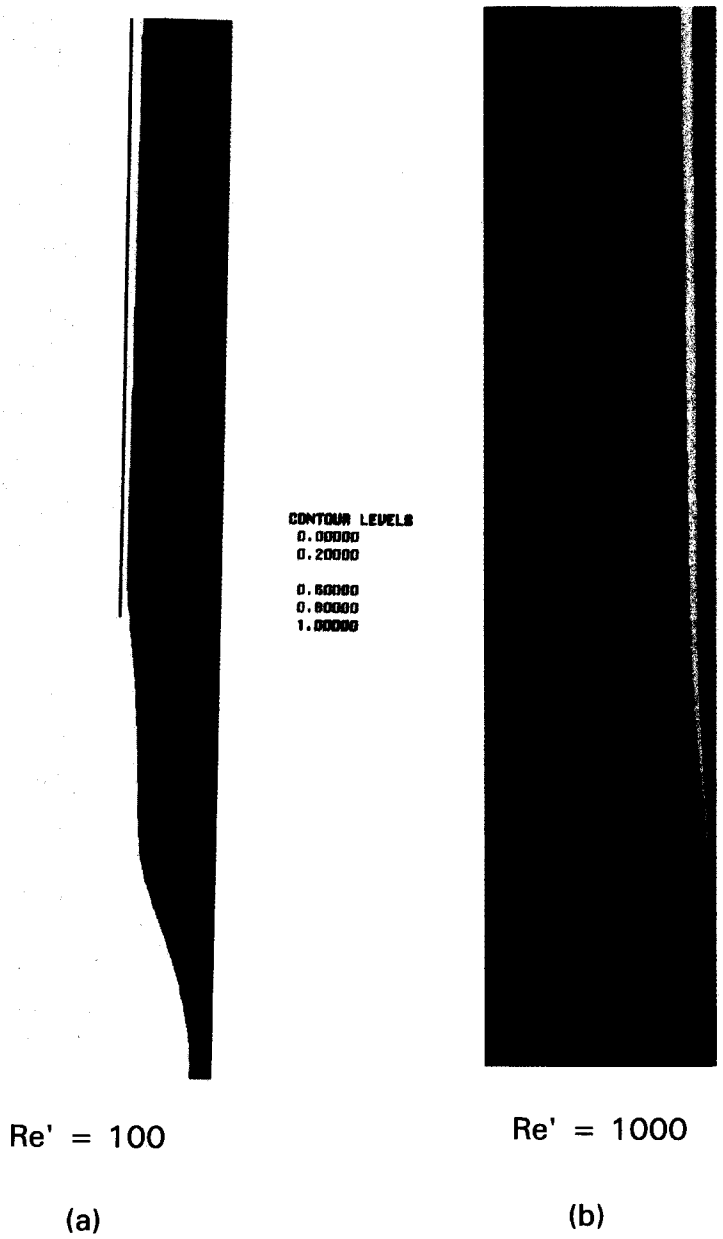

Fig. 5. Isotherms for $Re' = 100$ and $Re' = 1000$.

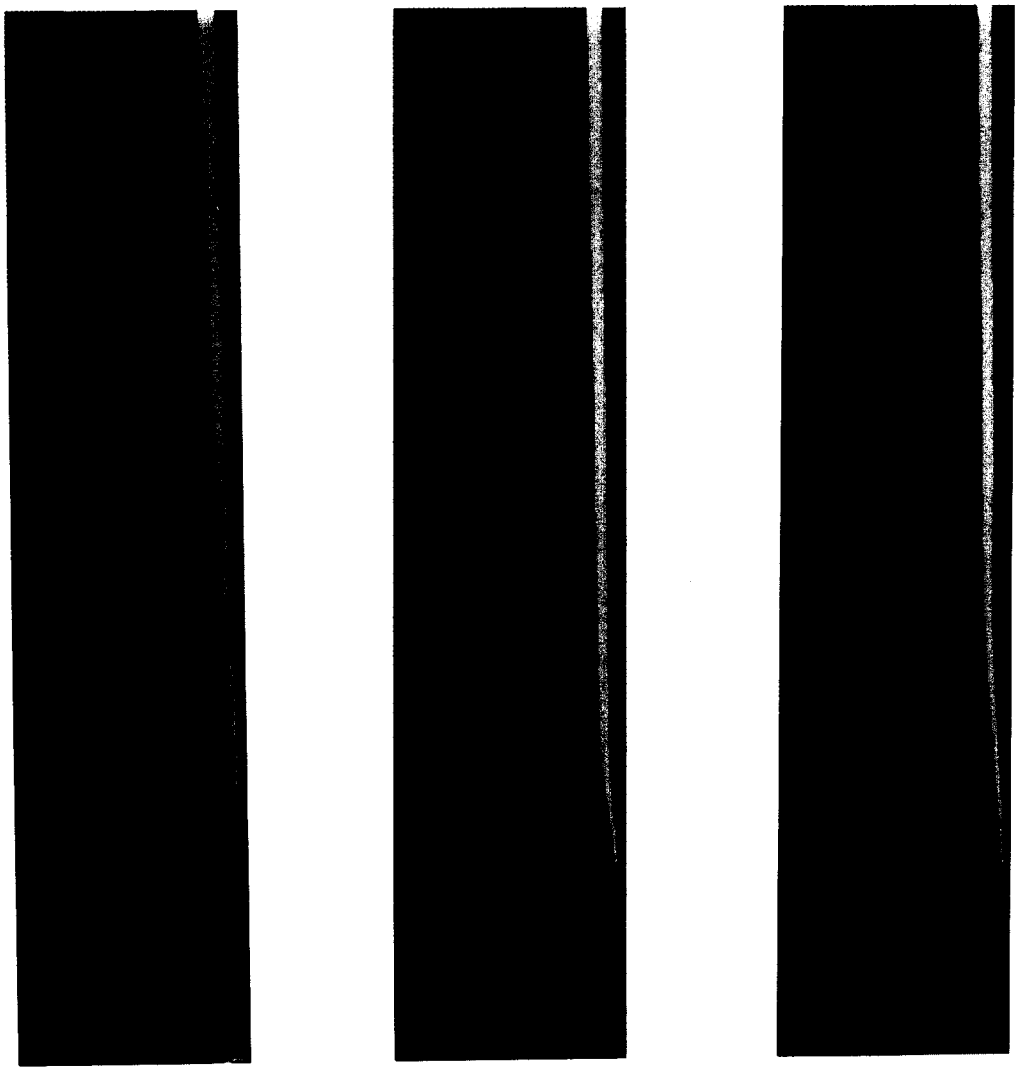

Fig. 9. Isotherms for $H/D = 0.1$, 0.5 and 2.0.

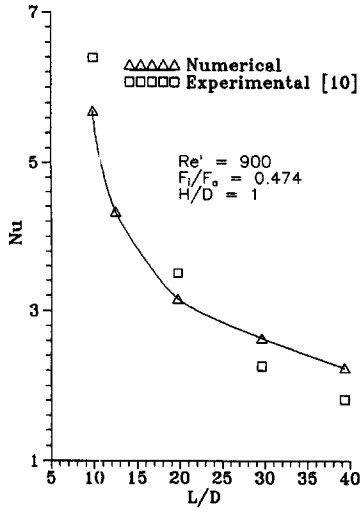

Fig. 6. Effect of length:diameter ratio on Nusselt number.

the Nusselt number decreases with increasing length: diameter ratio, consistent with the definition given earlier.

The numerical results lie within $\pm 10\%$ of the experimental data except at higher L/D values, where again the deviations are not very large.

4.3. *Effect of area ratio*

As evident from Fig. 7, the area ratio, F_i/F_a, does not affect the heat transfer rate significantly. The entire family of curves represent data in the range $2.85 < Nu < 4.25$, and the range is much smaller for a given value of H/D. The numerical and experimental data ($H/D = 1.0$) are again seen to agree within experimental error.

Considering the numerical curve for the "standard" clearance ratio ($H/D = 1.0$), a maximum is observed near $F_i/F_a \approx 0.47$. Since this area ratio corresponds to a stable axisymmetric vortex formed at minimum pressure drop in the hydraulic study [15], it represents a favourable design value. A decrease in heat transfer rate for area ratios below 0.47 may be attributed to reduced forced convection in the annulus. Because of a very high frictional loss, this range is of little practical importance [11, 15]. At much higher area ratios, lower heat transfer rates may again be expected; thermal penetration through the annulus into the incoming fluid then occurs, thus raising its temperature. The effect of three-dimensional (3D) flow [15] is evidently weak.

4.4. *Effect of clearance ratio*

The Nusselt number data for different clearance ratios are plotted in Fig. 8. The numerical and experimental data ($F_i/F_a = 0.474$) again agree within experimental error. Behaviour may be explained using the temperature profiles in Fig. 8.

For $F_i/F_a = 0.474$, at $H/D = 0.1$, a ring of separation on the outer surface of the inner tube is formed along with a secondary vortex in the tube corner [15]. As seen in Fig. 9, the secondary vortex creates a small high temperature zone at the outer tube bottom. Beyond $H/D = 0.5$, the ring of separation develops into a torodial vortex in the clearance zone; the secondary vortex subsides. The heat transfer rate is correspondingly decreased. At $H/D = 1.0$, the ring of separation has become a full detached ring vortex extending between the outer tube sealed end and the inner tube bottom [15]. The Nu vs H/D curve in Fig. 8 tends to flatten out. For H/D values greater than 1.0, a reduced circulation within this vortex, which no longer extends over the clearance zone, further reduces the heat transfer rate. Evidently, a lower value of H/D is favourable for thermal design; however, it may or may not produce a lower pressure loss [15].

4.5. *Effect of buoyancy*

Nusselt number data for different Rayleigh numbers is plotted in Fig. 10. As shown, the effect of Rayleigh number is small. This clearly indicates that the order of magnitude of the buoyancy term in the equation of motion is much smaller than the forced convection term for the range of Ra' considered, i.e. $10^{-5} < Ra'/(Re')^2 < 10^{-1}$. If the annular Rayleigh

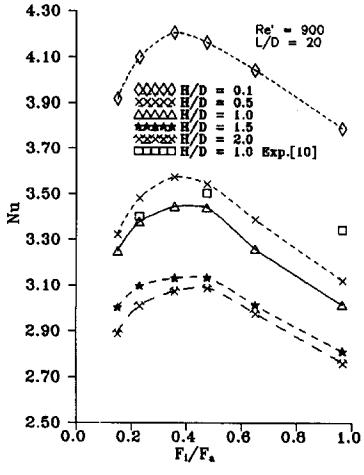

Fig. 7. Effect of area ratio on Nusselt number.

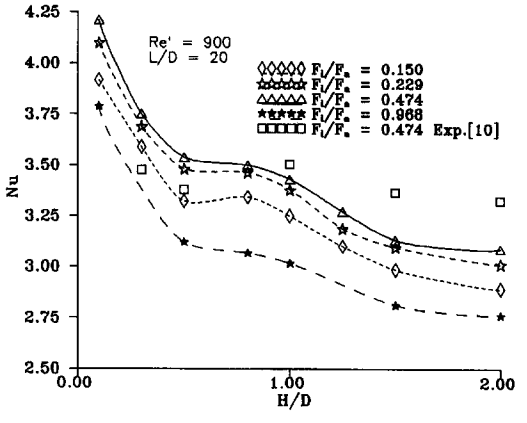

Fig. 8. Effect of clearance ratio on Nusselt number.

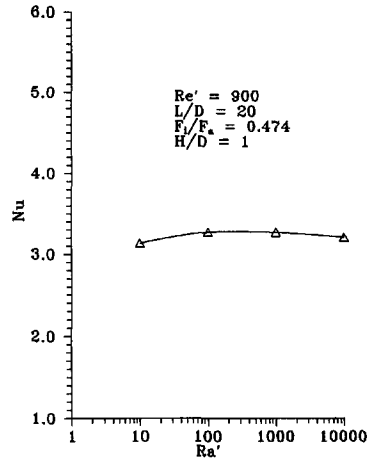

Fig. 10. Effect of Rayleigh number on Nusselt number.

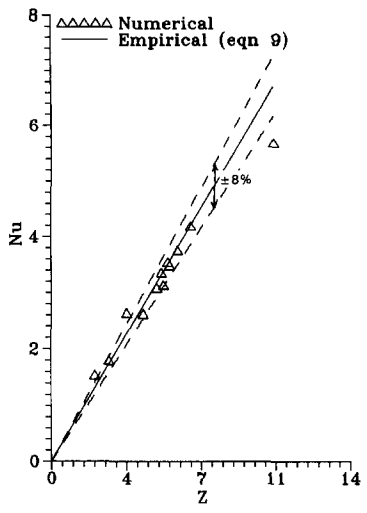

Fig. 11. Comparison with empirical heat transfer correlation.

number, Ra_a, obtained by replacing T_0 by T_b in equation (7), and the annular Reynolds number, Re_a, from ref. [11] are considered, then $Ra_a/(Re_a)^2 < 0.025$ for the range of Ra' plotted in Fig. 10.

4.6. *Correlation*

To construct a suitable correlation form it was decided at the outset that the effects of Reynolds number and length-diameter ratio could be represented by a power law, as suggested by Figs. 4 and 6. Higher heat transfer rate operation dictates the choice of function describing the effect of area ratio. An attempt was made to approximate the maximum seen in Fig. 7 by taking a simple parabolic form. An exponential fit was used for the effect of clearance ratio, but Fig. 8 reveals this to be only a rough approximation. However, for design purposes a more accurate curve fit may not be warranted. A general relationship was then constructed in the product form

$$Nu = 0.645Z \tag{9}$$

where Z was empirically determined as

$$Z = \left(\frac{D}{L}\right)^{0.98}\left[0.05+\left(0.7-\frac{F_i}{F_a}\right)^2\right]^{-0.07} \times \exp^{-0.073(H/D)} Re^{0.61} Ra^{0.05}.$$

Figure 11 shows numerical data from this study superimposed on the above correlation. The data almost all fall within a band of $\pm 8\%$, which is consistent with the overall uncertainty. This accuracy is acceptable for most applications of the bayonet tube. The correlation should thus be useful for a wide range of industrial and geotechnical problems.

5. CONCLUSIONS

The paper presents numerical data for heat transfer in a bayonet tube with laminar air flow. The results have been obtained for a constant property, steady flow in a cylindrical end bayonet tube. The results were plotted with Reynolds number, length:diameter ratio, area ratio, clearance ratio, and Rayleigh number as the independent variables and Nusselt number as the dependent variable. Parametric effects were examined in relation to velocity and temperature profiles. In general, good agreement with previous experimental data was demonstrated.

The Nusselt number was found to increase monotonically with Reynolds number, while the opposite was true for length:diameter ratio.

With respect to the effect of the area ratio, the maximum Nusselt number corresponded to the minimum pressure drop. For area ratios below the maximum, a reduced forced convection decreased heat transfer. For area ratios above the maximum, thermal penetration into the incoming fluid lowered *Nu*. With respect to the effect of the clearance ratio, examination of velocity and temperature profiles revealed a ring of separation along with a secondary vortex accounting for higher heat transfer at lower H/D values. A lower value of *Nu* for H/D values greater than 1.0 was attributed to the reduced effect of the stable end clearance vortex.

The negligible effect of Rayleigh number on Nusselt number was attributed to the relatively small magnitude of the buoyancy term in the axial momentum equation.

Acknowledgements—This work was made possible through the support of Natural Sciences and Engineering Research Council of Canada to whom we are indebted.

REFERENCES

1. G. S. H. Lock, *The Tubular Thermosyphon*. Oxford University Press, Oxford (1992).
2. H. O. Jahns, T. W. Miller, L. D. Power, W. P. Rickey, T. P. Taylor and J. A. Wheeler, Permafrost protection for pipelines on permafrost, *Proceedings 2nd International Conference on Permafrost*, pp. 673–684. National Academy Press (1973).
3. F. D. Haynes and J. P. Zarling, A comparative study of

thermosyphon used for freezing soil, ASME Paper #82-WA/HT (1982).
4. G. S. H. Lock, Control of spring run-off in northern rivers: the ice veil concept, *Polar Record*, pp. 451–457 (1986).
5. N. L. Hurd, Mean temperature difference in field or bayonet tube, *Ind. Engng Chem.* **38**(12), 1266–1271 (1946).
6. A. P. Fraas, A potassium-steam binary vapour cycle for better fuel economy and reduced thermal pollution, *J. Engng Power* **95**, 53–63 (1973).
7. Y. M. Zhang and H. W. Zhang, Experimental investigation of flow characteristics about tip heat transfer in bayonet tube (in Chinese), *Huagong Jixie* **15**(2), 96–102 (1988).
8. P. Hinchley, Key aspects of the design and specification of individual items of plant. In *Heat Exchanger Design Handbook* (Edited by B. A. Bolding and M. Prescott), Vol. 3, pp. 3.16.2-1 to 3.16.2-15. Hemisphere, Washington, D.C. (1984).
9. M. Luu and K. W. Grant, Thermal and fluid design of a bayonet tube heat exchanger for high-temperature waste heat recovery. In *Industrial Heat Exchangers* (Edited by A. J. Hayes, W. W. Wang, S. C. Richlen and E. S. Tabb), pp. 159–173 (1985).
10. G. S. H. Lock and Maolin Wu, Heat transfer characteristics of a bayonet tube using air under laminar conditions. *Int. J. Heat Mass Transfer* **36**(2), 287–291 (1993).
11. G. S. H. Lock and Maolin Wu, Laminar frictional behaviour of a bayonet tube, *Proceedings 3rd International Symposium on Cold Regions Heat Transfer*, pp. 429–440. Fairbanks, (1991).
12. S. V. Patankar, *Numerical Heat Transfer and Fluid Flow*. Hemisphere, Washington, DC (1980).
13. J. P. Van Doormaal and G. D. Raithby, Enhancement of the SIMPLE method for predicting incompressible fluid flows, *Numer. Heat Transfer* **7**, 147–163 (1984).
14. T. W. Jackson, W. B. Harrison and W. C. Boteler, Combined free and forced convection in a constant temperature vertical tube, *ASME Trans.* **86**, 739–745 (1964).
15. H. S. Minhas, The bayonet tube: a numerical analysis of laminar frictional characteristics, M.Sc. Thesis, University of Alberta, Edmonton, Alberta (1993).